

Carbon dynamics and export from flooded wetlands: A modeling approach



Amirreza Sharifi^a, Latif Kalin^{b,*}, Mohamed M. Hantush^c,
Sabahattin Isik^d, Thomas E. Jordan^e

^a School of Forestry and Wildlife Sciences, Auburn University, AL, United States

^b School of Forestry and Wildlife Sciences, Auburn University, 602 Duncan Dr., Auburn, AL 36849, United States

^c Land Remediation and Pollution Control Division, National Risk Management Research Laboratory, ORD, USEPA, United States

^d Engineering Faculty, Turgut Ozal University, Turkey

^e Smithsonian Environmental Research Center, United States

ARTICLE INFO

Article history:

Received 28 January 2013

Received in revised form 25 April 2013

Accepted 26 April 2013

Available online 15 June 2013

Keywords:

Wetlands

Model

Carbon

Methane

CH₄

DOC

Dissolved organic carbon

Carbon export

Greenhouse gas emission

Aerobic

Anaerobic

Diffusion

Ebullition

ABSTRACT

Described in this article is development and validation of a process based model for carbon cycling in flooded wetlands, called WetQual-C. The model considers various biogeochemical interactions affecting C cycling, greenhouse gas emissions, organic carbon export and retention. WetQual-C couples carbon cycling with other interrelated geochemical cycles in wetlands, i.e. nitrogen and oxygen; and fully reflects the dynamics of the thin oxidized zone at the soil–water interface. Using field collected data from a small wetland receiving runoff from an agricultural watershed on the eastern shore of Chesapeake Bay, we assessed model performance and carried out a thorough sensitivity and uncertainty analysis to evaluate the credibility of the model. Overall, model performed well in capturing TOC export fluctuations and dynamics from the study wetland. Model results revealed that over a period of 2 years, the wetland removed or retained equivalent to $47 \pm 12\%$ of the OC carbon intake, mostly via OC decomposition and DOC diffusion to sediment. The study wetland appeared as a carbon sink rather than source and proved its purpose as a relatively effective and low cost mean for improving water quality.

© 2013 Elsevier B.V. All rights reserved.

1. Introduction

Wetlands are environments characterized with waterlogged soils and biota adapted to saturated soil conditions. They are found in almost every climate and continent (with exception of Antarctica) and recognized for their unique role in regulating global biogeochemical cycles (Reddy and DeLaune, 2008).

In the context of global biogeochemical budgets, it is the carbon (C) cycle that wetlands influence the most. Because of high productivity and slow decomposition rates, wetlands have the highest carbon density among all terrestrial ecosystems (Kayranli et al., 2010). Despite covering less than 8% of the terrestrial land surface (Aselmann and Crutzen, 1989; Mitsch and Gosselink, 2007), wetlands are the greatest individual source of methane emission to the atmosphere (Walter and Heimann, 2000). Wetland methane

emissions have been estimated about 100–231 Tg CH₄ yr⁻¹ which accounts for 17–40% of the global (anthropogenic + natural) methane emissions annually (Denman et al., 2007). Influence of wetlands on global carbon balance is not limited to sequestering atmospheric carbon and emitting greenhouse gasses. When hydrologically connected to surface flow, wetlands export carbon in form of dissolved and particulate organic material (DOM and POM) to receiving waters (Reddy and DeLaune, 2008), acting as primary source of humic substances to freshwater aquatic systems (Stern et al., 2007; Ziegler and Fogel, 2003). Much of the organic material exported from wetlands eventually end up in oceans and it is estimated that 15% of the terrestrial organic matter flux to the oceans originate from wetlands (Hedges et al., 1997; Tranvik and Jansson, 2002).

Wetlands are widely referred to as “the kidneys of the catchment” due to their effectiveness in trapping sediment and nutrient loadings from surface waters (Mitchell, 1994; Mitsch and Gosselink, 2007). But the fact that wetlands can be net exporters of organic carbon (OC) potentially offsets their purifying benefits. Discharge of

* Corresponding author. Tel.: +1 334 844 4671; fax: +1 334 844 1084.

E-mail address: Latif@auburn.edu (L. Kalin).

carbon from wetlands will result in water quality degradation with the release of dissolved organic carbon (DOC), also known as water color (Worrall et al., 2003). At high concentrations, DOC reacts with chlorine during drinking water treatment to form carcinogenic disinfection byproducts (Chow et al., 2003). Also because of its hydrophobic nature, DOC is shown to be a medium of transport for other pollutants such as nutrients and heavy metals (Canário et al., 2008; Steinberg, 2003).

Because of the great influence of wetlands on global C cycling, and specifically considering the significant impact of wetlands greenhouse gas (GHG) emissions on global warming, considerable scientific efforts have been invested in quantifying wetland C storage, turnover, hydrologic exports and carbon interchanges between wetland soils and atmosphere. Wetland models have provided powerful tools for quantifying these budgets where field studies were not practical or projections for future budgets were called for. Various C cycling models have been developed for wetlands over the past three decades (Mitsch et al., 1988). Although these models varied in scale of application (temporally and spatially), complexity and approach (empirical vs. physically based) they all roughly targeted similar objectives. These objectives were to (1) synthesize our knowledge of complex interactions between wetland soil, hydrology and vegetation; and (2) assess, quantify and predict impacts of climate change or management alternatives on C dynamics, storage and export from wetlands (Cui et al., 2005; Zhang et al., 2002). Existing wetland C models can generally be classified into various categories based on the final specific product of the C cycle that they are geared to simulate. These categories can be confined to long term-peat accumulation related models, greenhouse gas (CH_4 and CO_2) emission models and wetland OC turnover and export models. Models falling into the last category are more or less specific to treatment wetlands (e.g. King et al., 2003; Penha-Lopes et al., 2012 and Stern et al., 2007). Wetland GHG emission models have received the most attention among all categories in recent years. Among the latest and most comprehensive models in this category is the work of Tang et al. (2010) where they revised a previously developed geochemistry model (TEM model, Zhuang et al., 2004) into a multi substance model to simulate methane production, oxidation and transport with different model complexities. The model uses a probabilistic algorithm to account for the effects of hydrostatic pressure on ebullition. At the most complex, the model considers four substances (O_2 , N_2 , CO_2 and CH_4) and accounts for the inhibitory effect of O_2 on CH_4 production and the stimulatory effect of O_2 on CH_4 oxidation. At the simplest, the model was reduced to a one substance system (CH_4 only) by ignoring the role of O_2 . The authors concluded that the four substance model predicted the effects of atmospheric pressure and water table dynamics on methane effluxes more accurately than simpler tested models. Another recent methane model development, designed for large-scale simulation of CH_4 emissions from northern peatlands, is described by Wania et al. (2010). The methane model takes into account the interactions between hydrology, soil temperature and vegetation leading to methane production and emission. The model was integrated into a dynamic global vegetation model and applied to various peatland sites. Despite the fact that the model setup does not require site-specific input data, it performs reasonably well in predicting methane production and emission from northern peatlands.

The purpose of this paper was to develop a physically based model for carbon cycling and methane production in flooded wetlands. As stated earlier, many of the existing wetland water quality models focus on a single end product of the carbon cycle, i.e. methane production, OC export or OC deposition. In this study, we aim to advance the current state of wetland modeling by introducing a computationally simple – yet comprehensive – mechanistic wetland carbon cycling model. The proposed model in this study

reflects various biogeochemical interactions affecting C cycling in wetlands, and is capable of simulating the dynamics of OC retention, OC export and GHG emissions. What makes this model special is the fact that it is coupled with other interrelated geochemical cycles (i.e. nitrogen and oxygen) and fully reflects the dynamics of sediment–water interactions in flooded wetlands. Another unique aspect of the developed model is its approach towards modeling the formation of the thin oxidized zone at wetlands soil–water interface and the oxidation–reduction reactions taking place within that zone (Mitsch and Gosselink, 2007; Reddy and DeLaune, 2008). We perform a thorough sensitivity and uncertainty analysis on model components to validate its credibility using field collected data from a small wetland that receives runoff from an agricultural land. In the following sections of the paper, we describe the structure of the model and the methodology on model assessment. Finally the results are presented and discussed.

2. Model description

2.1. WetQual-C model

WetQual-C model is an extension to WetQual model, a previously developed wetland nutrient cycling model (Hantush et al., 2012). WetQual is a process based model for nitrogen and phosphorus retention, cycling, and removal in flooded wetlands. The model simulates oxygen dynamics and impact of oxidizing and reducing conditions on nitrogen transformation and removal as well as phosphorus retention and release. WetQual explicitly accounts for nitrogen loss pathways of volatilization and denitrification. The model separates free floating plant biomass (e.g., phytoplankton) from rooted aquatic plants and uses a simple model for productivity in which daily growth rate is related to daily solar radiation and annual growth rate of plants. In developing WetQual-C, we followed the same compartmental structure as WetQual, where a wetland is partitioned into two basic compartments; the water column (free-water) and wetland soil layer. The soil layer is further partitioned into a generalized model of aerobic and anaerobic zones where the boundary between the two zones fluctuates up or down based on competing oxygen supply and removal rates. To reflect the complex cycling of organic matter and methane production in flooded wetlands, it was necessary to posit several organic and inorganic carbon pools within WetQual-C model. As can be viewed in Fig. 1, two pools for particulate organic carbon (POC) are considered in the model, one representing fast reacting, easily degradable organic material (e.g. non-humic substances, carbohydrates) and the other describing recalcitrant, slow reacting solids (e.g. phenolic and humic substances). The former pool is called labile particulate organic carbon (LPOC) and the latter pool is referred to as refractory particulate organic carbon (RPOC). A third organic pool represents dissolved organic carbon (DOC). Model allows for allochthonous sources to contribute to all three organic pools. If wetland is hydrologically connected to surface flow, or is intended as means for treating water, a significant amount of external organic C can be transferred into the system via incoming flow, originating from point sources (e.g. sewage pipes) or diffuse source upland areas (e.g. agricultural fields). An internal source for DOC and POC includes plant matter from emergent macrophytes, algal mats and litter fall from trees in forested wetlands.

A stepwise conversion process is considered in the model to portray all stages of plant turnover and OM decomposition. When plants senesce, part of their biomass leaches out physically in form of water soluble–highly labile–organic compounds (Reddy and DeLaune, 2008). Within each compartment in the model (water and sediment), this portion of the biomass is directly added to the

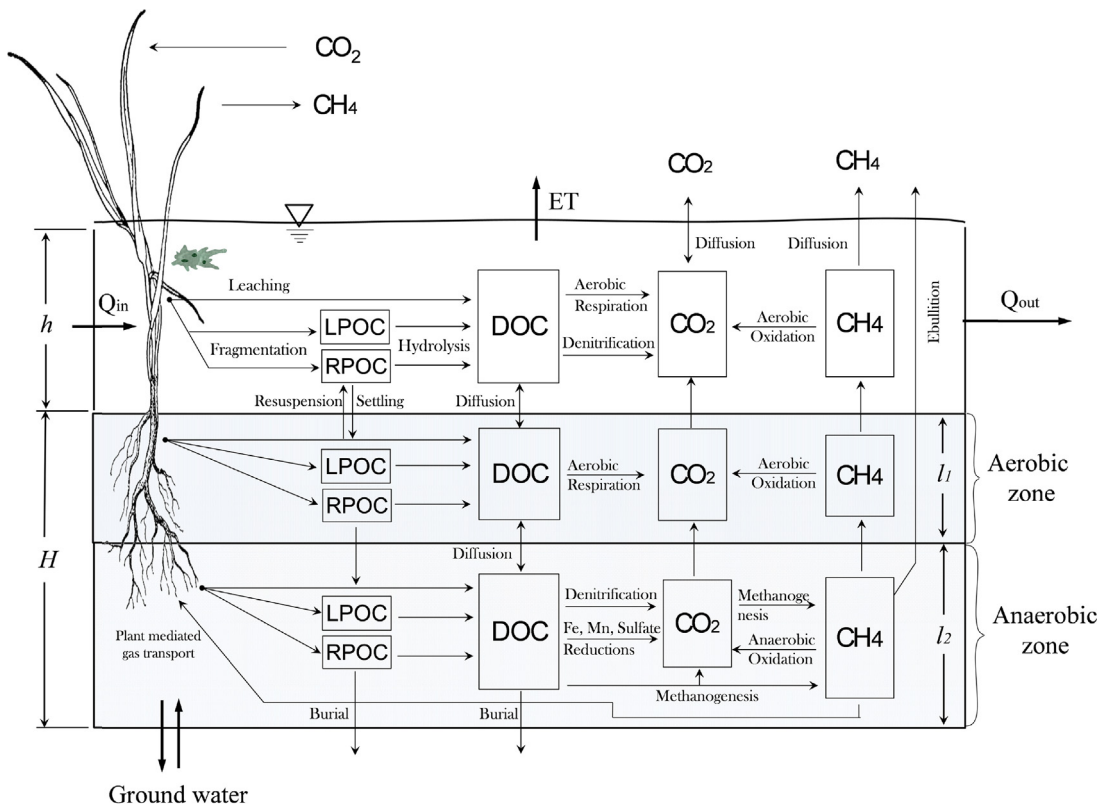


Fig. 1. Conceptual model for carbon cycling in flooded wetlands. The wetland is partitioned into two layers: water and sediment. Sediment layer is further partitioned into aerobic and anaerobic (reduced) zones. The boundary between the two sediment zones fluctuates up or down dynamically based on sediment and water oxygen demands.

DOC pool. Rest of the biomass (detritus) is fragmented between LPOC and RPOC pools with split ratios depending on type of plant and quality of detritus. Parts of the plants with higher biodegradability and low in lignin content are directed to LPOC pool, whereas more stable fragments, such as conductive and supportive tissue cells, are allocated to RPOC pool. In a process called hydrolysis, complex high molecular-weight organic matters are broken down into smaller and simpler compounds. This process is mediated by extra-cellular enzymes released by microorganisms (bacteria and fungi) living in soil and on the surface of plants. In the model, hydrolysis process affects LPOC and RPOC pools, such that they gradually decay and turn into DOC. In the model, LPOC and RPOC hydrolysis rates are temperature dependent, however, on average, LPOC hydrolysis rate is about 10 times faster than RPOC in the model (Cerco and Cole, 1995; Reddy and DeLaune, 2008). This difference makes RPOC in water column more prone to settling and burial whereas LPOC can decompose partly in water. In natural wetlands, burial is a potential loss pathway caused by net sedimentation. This important process has significant long-term impact on OC mass balance (e.g., at the annual time scale or decades). Burial is considered in WetQual-C by moving the water-soil interface upward. In other words, both particulate and dissolved pore-water constituents are moving downward with a velocity equal to the burial rate relative to an upward moving soil water interface.

At the last step of decomposition, simpler organic compounds are assimilated, oxidized and turned into inorganic molecules, mainly CO_2 , by heterotrophic microorganisms. In the water column and the aerobic sediment layer, where oxygen is abundant, aerobic heterotrophs dominate decomposition and release CO_2 . In anaerobic sediment layer and in the absence of oxygen, dominant microbial groups are anaerobes. Depending on availability of electron acceptors (oxidants) in wetland soil (e.g. NO_3^- , Mn^{4+} , Fe^{3+} , SO_4^{2-}), different communities of anaerobes oxidize simple

organic molecules and release carbon dioxide. Methane is only produced when all other electron acceptors are reduced in wetland soil (Mitsch and Gosselink, 2007). This process is called methanogenesis and is performed by a group of microbes named methanogens, commonly using CO_2 as electron acceptor (Reddy and DeLaune, 2008). WetQual-C considers DOC pool as potential reservoir for oxic and anoxic/anoxic respiration.

2.2. Mass balance equations

The mass balance equations presented below account for the processes, interactions and loss pathways for organic and inorganic carbon in a typical flooded wetland. The equations are in form of ordinary differential equations and solved numerically using an explicit scheme with forward difference approximation. In the following section, mass balance relationships for organic C pools in water and sediment columns are expressed first. Following that, we present relationships employed in WetQual-C model for dynamic simulation of inorganic C pools (methane in water and sediment columns).

2.2.1. Organic C Water Column:

$$\phi_w \frac{d(V_w C_{Lw})}{dt} = Q_{in} C_{Li} + a_{ca} k_{da} f_{aL} a + a_{ca} k_{db} f_{bw} f_{bL} b - \phi_w V_w k_L C_{Lw} - Q_o C_{Lw} - v_s \phi_w A C_{Lw} + v_r \phi_w A C_{L1} \quad (1)$$

$$\phi_w \frac{d(V_w C_{Rw})}{dt} = Q_{in} C_{Ri} + a_{ca} k_{da} f_{aR} a + a_{ca} k_{db} f_{bw} f_{bR} b - \phi_w V_w k_R C_{Rw} - Q_o C_{Rw} - v_s \phi_w A C_{Rw} + v_r \phi_w A C_{R1} \quad (2)$$

$$\begin{aligned} \varphi_w \frac{d(V_w C_{Dw})}{dt} = & Q_{in} C_{Di} + a_{ca} k_{da} f_{ad} a + a_{ca} k_{db} f_{bw} f_{bd} b + \varphi_w V_w k_L C_{Lw} \\ & + \varphi_w V_w k_R C_{Rw} - Q_o C_{Dw} + F_{C_{Dg}}^w + \beta_{D1} A(C_{D1} - C_{Dw}) \\ & - \varphi_w V_w \frac{O_w}{O_w + K_O} k_D^1 C_{Dw} \\ & - \varphi_w V_w \frac{K_O^{in}}{O_w + K_O^{in}} \frac{N_{nw}}{N_{nw} + K_N} k_D^2 C_{Dw} \end{aligned} \quad (3)$$

in which

$$F_{C_{Dg}}^w = \begin{cases} Q_g C_{D1}, & Q_g > 0 \\ Q_g C_{Dw}, & Q_g < 0 \end{cases} \quad (4)$$

where C_{Lw} , C_{Rw} and C_{Dw} , respectively, are concentrations of labile (fast reacting) particulate organic C (LPOC), refractory (slow reacting) particulate organic C and dissolved organic C in free water [ML^{-3}]; a is mass of free floating and attached plants [$M Chl a$]; b is mass of rooted plants [$M Chl a$]; C_{L1} , C_{R1} and C_{Di} are respectively concentrations of LPOC, RPOC and DOC in incoming flow [ML^{-3}]; C_{L1} , C_{R1} and C_{Di} are pore water concentrations of LPOC, RPOC and DOC in aerobic sediment layer, respectively [ML^{-3}]; v_s and ν_r are effective settling and resuspension rates for organic material in water [LT^{-1}]; V_w is water volume of wetland surface water [L^3]; A is wetland surface area [L^2]; Q_i is volumetric inflow rate [$L^3 T^{-1}$]; Q_o is wetland discharge (outflow) rate [$L^3 T^{-1}$]; $F_{C_{Dg}}^w$ is groundwater source/loss for DOC [MT^{-1}] and Q_g is groundwater flow [LT^{-3}] that can be either positive (upwards-discharging to the wetland) or negative (downwards-recharging groundwater table). O_w and N_{nw} are, respectively, concentration of oxygen and NO_3^- in water column. Since plant biomass occupies part of submerged wetland volume, we defined φ_w as effective porosity of wetland surface water to account for such effects. Other related biochemical parameters and reaction rates applied in WetQual-C formulation are defined in Table 1. When oxygen is present in water, aerobic heterotrophs dominate microbial decomposition. Thus, as appears in Eq. (3), oxic respiration is the dominant reaction when oxygen is abundant in water column. When oxygen is depleted from water, the model allows for denitrification in water column. In freshwater wetlands, it is safe to assume that redox potential does not drop below 100 mV in water column (Reddy and DeLaune, 2008), thus, the lowest redox reaction allowed in water column is denitrification. Using Michaelis-Menten kinetics, the rate of aerobic DOC oxidation is limited by oxygen levels (concentration) in water. K_O is half saturation concentration of oxygen for aerobic respiration, equivalent to a concentration of O_2 at which aerobic respiration rate is half of its maximum (k_D^1). Similarly, denitrification of DOC (last term on right hand side of Eq. (3)) is limited by both nitrate and oxygen concentrations. Michaelis-Menten coefficients of K_O , K_O^{in} and K_N are used as calibration parameters throughout most DOC and CH_4 related equations.

Aerobic Sediment Layer:

$$\begin{aligned} V_{s1} \frac{dC_{L1}}{dt} = & a_{ca} k_{db} f_1 f_{bs} f_{bl} b - V_{s1} k_L C_{L1} + f_1 \varphi_w v_s A C_{Lw} \\ & - f_1 \nu_r A C_{L1} - \nu_b A C_{L1} \end{aligned} \quad (5)$$

$$\begin{aligned} V_{s1} \frac{dC_{R1}}{dt} = & a_{ca} k_{db} f_1 f_{bs} f_{br} b - V_{s1} k_R C_{R1} + f_1 \varphi_w v_s A C_{Rw} - f_1 \nu_r A C_{R1} \\ & - \nu_b A C_{R1} \end{aligned} \quad (6)$$

$$\begin{aligned} \phi V_{s1} \frac{dC_{D1}}{dt} = & a_{ca} k_{db} f_1 f_{bs} f_{bd} b + V_{s1} k_L C_{L1} + V_{s1} k_R C_{R1} \\ & - B_{D1} A(C_{D1} - C_{Dw}) - \beta_{D2} A(C_{D1} - C_{D2}) + F_{C_{Dg}}^1 \\ & - \phi V_{s1} \frac{O_{s1}}{O_{s1} + K_O} k_D^1 C_{D1} - \phi \nu_b A C_{D1} \end{aligned} \quad (7)$$

in which

$$F_C^{Dg} = \begin{cases} Q_g C_{D2} - Q_g C_{D1}, & Q_g > 0 \\ Q_g C_{D1} - Q_g C_{Dw}, & Q_g < 0 \end{cases} \quad (8)$$

where V_{s1} is volume of aerobic sediment layer ($V_{s1} = l_1 \times A_w$) [L^3]; C_{D2} is pore water concentration of DOC in lower anaerobic sediment layer [ML^{-3}], O_{s1} is oxygen concentration in aerobic sediment ($O_{s1} = O_w/2$) and $F_{C_{Dg}}^1$ is groundwater source/loss of DOC from aerobic sediment layer [MT^{-1}]. Eq. (9) defines the thickness of the top oxic soil layer [L]:

$$l_1 = -\phi \tau \delta + \sqrt{(\phi \tau \delta)^2 + \frac{2\phi \tau D_o^* O_w}{\Omega}} \quad (9)$$

where O_w is oxygen concentration in free water [ML^{-3}], δ is the thickness of a laminar (diffusive) boundary layer situated on top of the soil-water interface [L] ($\delta \approx h/2$ for shallow wetland waters); τ is the wetland soil tortuosity factor; D_o^* is free-water oxygen diffusion coefficient [$L^2 T^{-1}$] and Ω is oxygen removal rate per unit volume of aerobic soil layer [$ML^{-3} T^{-1}$]. Once l_1 is computed, the thickness of the lower anoxic layer would be $l_2 = H - l_1$ where H is the thickness for active sediment layer [L]. Refer to Hantush et al. (2012) for more details on oxygen dynamics in WetQual model. Definitions for rest of the parameters are either presented earlier or could be found in Table 1.

Anaerobic Sediment Layer:

$$\begin{aligned} V_{s2} \frac{dC_{L2}}{dt} = & a_{ca} k_{db} f_2 f_{bs} f_{bl} b - V_{s2} k_L C_{L2} + f_2 \phi_w v_s A C_{Lw} - f_2 \nu_r \phi_w A C_{L2} \\ & - \nu_b A(C_{L2} - C_{L1}) \end{aligned} \quad (10)$$

$$\begin{aligned} V_{s2} \frac{dC_{R2}}{dt} = & a_{ca} k_{db} f_2 f_{bs} f_{br} b - V_{s2} k_R C_{R2} + f_2 \phi_w v_s A C_{Rw} \\ & - f_2 \nu_r \phi_w A C_{R2} - \nu_b A(C_{R2} - C_{R1}) \end{aligned} \quad (11)$$

$$\begin{aligned} \phi V_{s2} \frac{dC_{D2}}{dt} = & a_{ca} k_{db} f_2 f_{bs} f_{bd} b + V_{s2} k_L C_{L2} + V_{s2} k_R C_{R2} \\ & - \beta_{D2} A(C_{D2} - C_{D1}) + F_{C_{Dg}}^2 - \phi \nu_b A(C_{D2} - C_{D1}) \\ & - \phi V_{s2} \frac{N_{n2}}{N_{n2} + K_N} k_D^2 C_{D2} - \phi V_{s2} \frac{K_N^{in}}{N_{n2} + K_N^{in}} k_D^3 C_{D2} \end{aligned} \quad (12)$$

in which

$$F_C^{Dg} = \begin{cases} Q_g C_g - Q_g C_{s2}, & Q_g > 0 \\ Q_g C_{s2} - Q_g C_{s1}, & Q_g < 0 \end{cases} \quad (13)$$

where V_{s2} is volume of aerobic sediment layer ($V_{s2} = l_2 \times A_w$) [L^3]; C_{L2} and C_{R2} are pore water concentrations of LPOC and RPOC in lower anaerobic sediment layer respectively [ML^{-3}]; $F_{C_{Dg}}^2$ is groundwater source/loss of DOC from anaerobic sediment layer [MT^{-1}].

Since resuspension is a purely hydrodynamic process and independent of the soil redox condition, we allow resuspension from the entire active soil layer rather than limiting LPOC and RPOC

Table 1
WetQual-C model parameter definitions.

| Symbol | Definition | Dimension unit |
|--------------------------|--|---------------------------|
| a_{ca} | Ratio of carbon to chlorophyll-a in algae | MM^{-1} |
| a_{mc} | The stoichiometric yield of Methane from the anaerobic decomposition of a gram of organic carbon during methanogenesis | MM^{-1} |
| β_{D1}, β_{M1} | Diffusive mass-transfer rates, respectively, of DOC and CH_4 between wetland water and aerobic soil layer (see appendix B for details) | LT^{-1} |
| β_{D2}, β_{M2} | Diffusive mass-transfer rates, respectively, of DOC and CH_4 between wetland water and lower anaerobic soil layer (see appendix B for details) | LT^{-1} |
| C^* | Equilibrium concentration of CH_4 in atmosphere | ML^{-3} |
| D^σ | Diffusivity of Methane in air | L^2T^{-1} |
| D_M^*, D_D^* | Diffusivity of methane and DOC in water, respectively | L^2T^{-1} |
| f_1 | Volumetric fraction of the active soil layer that is aerobic $f_1 = \frac{l_1}{l_1+l_2}$ | Dimensionless |
| f_2 | Volumetric fraction of the active soil layer that is anaerobic $f_2 = \frac{l_2}{l_1+l_2}$ | Dimensionless |
| f_{al}, f_{aR}, f_{aD} | Fraction of, respectively, labile particulate, refractory particulate and dissolved organic C produced by death/loss of free floating plants and attached algae ($f_{al} + f_{aR} + f_{aD} = 1$) | Dimensionless |
| f_{bl}, f_{bR}, f_{bD} | Fraction of, respectively, labile particulate, refractory particulate and dissolved organic C produced by death/loss of rooted and benthic plants ($f_{bl} + f_{bR} + f_{bD} = 1$) | Dimensionless |
| f_{bw}, f_{bs} | Fraction of rooted plant biomass, respectively, above and under soil-water interface | Dimensionless |
| H | Thickness of active soil layer $H = l_1 + l_2$ | L |
| h | Average depth of water in wetland | L |
| J_M | Methane mass exchange coefficient between water and atmosphere | LT^{-1} |
| k_D^1, k_D^2, k_D^3 | Maximum dissolved organic C utilization rate for, respectively, aerobic respiration, denitrification and methanogenesis | T^{-1} |
| k_M^1, k_M^2 | Maximum methane utilization rate for, respectively, aerobic respiration and denitrification | T^{-1} |
| k_{da} | Death rate of free floating plants | T^{-1} |
| k_{db} | Death rate of rooted and benthic plants | T^{-1} |
| K_O^{in} | Michaelis–Menten oxygen inhabitation coefficient | ML^{-3} |
| K_N^{in} | Michaelis–Menten nitrate-N inhibition coefficient | ML^{-3} |
| k_L, k_R | First order hydrolysis rate of labile particulate organic carbon and refractory particulate organic carbon, respectively | T^{-1} |
| K_N | Michaelis–Menten nitrate N half saturation concentration required for denitrification | ML^{-3} |
| K_O | Michaelis–Menten half saturation concentration of dissolved oxygen required for oxic respiration | ML^{-3} |
| l_1, l_2 | Thickness of aerobic and anaerobic sediment layers | L |
| $S_C M$ | Schmidt number of methane | Dimensionless |
| S_B | Bunsen solubility coefficient for methane | Dimensionless |
| v_r | Resuspension/recycling rate of particulate organic C | LT^{-1} |
| v_s | Settling loss rate of particulate organic C | LT^{-1} |
| θ | Temperature coefficient in Arhenius equation. (see appendix A for parameters that are adjusted with temperature) | Dimensionless |
| λ_r | Specific conductivity of root system | LL^{-1} |
| τ | Tortuosity of sediment | Dimensionless |
| ϕ | Porosity of sediment | Dimensionless |
| ϕ_w | Effective porosity of wetland surface water | Dimensionless |

resuspension to the top aerobic soil compartment. Each of the soil compartments contributes an amount proportional to its respective thickness.

2.2.2. Methane-C (CH_4)

Before being released to the atmosphere, methane produced in reduced wetland soil is subjected to several geochemical and physical transformations. Methane emission to atmosphere is a balance between methane production, oxidation and transport within the soil and water (Bradford et al., 2001; Chan and Parkin, 2000; Reddy and DeLaune, 2008; Wania et al., 2010). Methane is transported to atmosphere via three different pathways of (1) plant aided diffusive exchange via aerenchyma of plants roots and stands (2) molecular diffusive flux through soil and water (3) abrupt elimination in form of bubbles (ebullition). Much of the transferred methane through molecular diffusion (up to 90%) and plant aided exchange (up to 50%) is oxidized to carbon dioxide by methanotrophic bacteria that consume methane as carbon and energy source (King, 1992; Reddy and Schipper, 1996). This fact reveals the importance of ebullition as major processes that regulate methane emission into the atmosphere. Ebullition may account for 30–85% of the total methane release from wetlands (Byrnes et al., 1995; Reddy and DeLaune, 2008). To capture the complicated cycle of methane, a robust model shall include proper equations to represent all processes related to

methane production, transfer and consumption. Since methane is generally produced in reduced soil and transferred upwards, we present methane mass balance equations in sediment layers first and then move upwards to water layer.

Sediment Columns:

Methane in sediment columns are simulated in a two-step process. In step one, processes other than ebullition (diffusion, oxidation, advective transport and plant mediated transport) are considered to define methane concentration. If methane concentration calculated in step one exceeds a certain partial pressure, the excess is transferred upwards to the atmosphere in form of bubbles (ebullition). This method is similar to approaches suggested by Kellner et al. (2006) and Wania et al. (2010). For anaerobic and aerobic sediment layers, the mass balance equations form as follows:

$$\begin{aligned} \varphi V_{s2} \frac{dC_{M2}}{dt} &= a_{mc} \varphi V_{s2} \frac{K_N^{in}}{N_{n2} + K_N^{in}} k_D^3 C_{D2} + \beta_{M2} A (C_{M1} - C_{M2}) \\ &\quad - \varphi V_{s2} \frac{N_{n2}}{N_{n2} + K_N^{in}} k_M^2 C_{M2} + F_{C_{Mg}}^2 \\ &\quad + \lambda_r f_2 f_{bs} b R_v D^\sigma (C^* - C_{M2}) \end{aligned} \quad (14)$$

Table 2
Model parameters with fixed values (i.e. constants).

| Parameter | Value |
|---------------------------------------|--------|
| a_{mc} (gr CH ₄ /gr DOC) | 0.267 |
| λ_r (m root/m soil) | 0.0003 |

$$\begin{aligned} \phi V_{s1} \frac{dC_{M1}}{dt} &= \beta_{M1} A(C_{Mw} - C_{M1}) + \beta_{M2} A(C_{M2} - C_{M1}) \\ &- \phi V_{s1} \frac{O_{s1}}{O_{s1} + K_O} k_M^1 C_{M1} + F_{C_{Mg}}^1 \\ &+ \lambda_r f_1 f_{bs} b R_v D^\sigma (C^* - C_{M1}) \end{aligned} \quad (15)$$

if $C_{Mi} > C_{Mi}^{eq}$ ($i = 1, 2$) then

$$\left\{ J_{Ebul}^{Mi} = \frac{(C_{Mi} - C_{Mi}^{eq}) \phi V_{si}}{\Delta t A} \text{ and } C_{Mi} = C_{Mi}^{eq} \right. \quad (16)$$

in which

$$F_{C_{Mg}}^2 = \begin{cases} -Q_g C_{M2}, & Q_g > 0 \\ Q_g C_{M2} - Q_g C_{M1}, & Q_g < 0 \end{cases} \text{ and}$$

$$F_{C_{Dg}}^1 = \begin{cases} Q_g C_{M2} - Q_g C_{M1}, & Q_g > 0 \\ Q_g C_{M1} - Q_g C_w, & Q_g < 0 \end{cases} \quad (17)$$

where C_{M2} , C_{M1} and C_w are methane concentration in anaerobic sediment, aerobic sediment layer and water, respectively [ML⁻³]; a_{mc} is the stoichiometric yield of Methane from the anaerobic decomposition of a gram of organic carbon during methanogenesis [MM⁻¹] (see Table 2 for constant value), β_{M2} is methane mass exchange coefficient between aerobic and anaerobic sediment [LT⁻¹]; β_{M1} is methane mass exchange coefficient between aerobic sediment and water [LT⁻¹]; k_D^3 is first-order reaction rate for DOC consumption by methanogenesis in reduced soil [T⁻¹]; k_M^2 is first order reaction rate for methane consumption via denitrification [T⁻¹]; k_M^1 is first order reaction rate for aerobic methane oxidation [T⁻¹] and $F_{C_{Mg}}^1$ and $F_{C_{Mg}}^2$ are groundwater source/loss for methane [MT⁻¹]. Groundwater is more likely to be a sink for methane rather than a source; however, some studies indicate that methane in ground water resources can constitute a significant pool of carbon (Barker and Fritz, 1981). Last term on right hand side of Eq. (14) and Eq. (15) account for plant mediated transfer of methane to atmosphere. Plant aided transfer of methane is assumed to be a function of root density and methane concentration gradient between soil and air (Yu et al., 1997). Following Tang et al. (2010), C^* is equilibrium concentration of CH₄ in atmosphere [ML⁻³], λ_r is specific conductivity of root system [LL⁻¹] (see Table 2 for constant value), R_v is root length density in soil [L root/M chla]; D^σ is diffusivity of methane in air [L²T⁻¹] (see appendix A for relationship of D^σ with temperature) and C^* is equilibrium concentration of CH₄ in atmosphere [ML⁻³] (see Appendix A for details).

C_{Mi}^{eq} [ML⁻³] is an upper limit for concentration of dissolved methane for sediment layer i ($i = 1, 2$) in which solubility of CH₄ is maximum. Such concentration for both sediment layers is obtained by combining Bonsen solubility coefficient of methane and ideal gas law (Wania et al., 2010):

$$C_{Mi}^{eq} = \frac{p_i}{RT} (S_B) \quad (18)$$

where T is the ambient water temperature (K), R is the universal gas constant (8.3145 m³ Pa K⁻¹ mol⁻¹), S_B is the Bunsen solubility coefficient, defined as maximum volume of gas dissolved per volume of liquid at given temperature and pressure (see Appendix

A for a temperature dependent relationship of S_B). p_i (unit: Pa) is the sum of atmospheric and hydrostatic pressures for sediment layer i ($p_i = p_{atm} + \rho g z$) where g is gravitational acceleration [LT⁻²], ρ is density of water [ML⁻³] and z is average water height over sediment layer [L]:

$$z = \begin{cases} h + \frac{l_1}{2} & i = 1 \\ h + l_1 + \frac{l_2}{2} & i = 2 \end{cases} \quad (19)$$

Excessive methane over maximum solubility is promptly cast out of the sediment layers via ebullition such that concentration of methane never exceeds the maximum limit. J_{Ebul}^M represents the flux of methane released by bubbling at each time step [ML⁻²T⁻¹].

Water Column:

$$\begin{aligned} \varphi_w \frac{d(V_w C_{Mw})}{dt} &= \alpha_M \varphi_w A(C^* - C_{Mw}) + \beta_{M1} A(C_{M1} - C_{Mw}) + F_{C_{Mg}}^w \\ &- Q_o C_{Mw} - \varphi_w V_w \frac{O_w}{O_w + K_O} k_M^1 C_{Mw} \\ &- \varphi_w V_w \frac{K_O^{in}}{O_w + K_O^{in}} \frac{N_{nw}}{N_{nw} + K_N} k_M^2 C_{Mw} \end{aligned} \quad (20)$$

in which

$$F_{C_{Mg}}^w = \begin{cases} Q_g C_{M1} & Q_g > 0 \\ Q_g C_{Mw} & Q_g < 0 \end{cases} \quad (21)$$

where, C_{Mw} is methane concentration in water [ML⁻³]; α_M is methane gas transfer velocity between water and atmosphere [LT⁻¹]; $F_{C_{Dg}}^w$ is groundwater source/loss for methane [MT⁻¹]. α_M , also referred to as piston velocity, is empirically derived using inert tracer gases and is usually related to wind speed over water (Wanninkhof et al., 2009). A variety of relationships for gas transfer velocities have been presented by Wanninkhof et al. (2009). The following relationship, valid for wind speeds less than 3.6 m s⁻¹, was selected for methane:

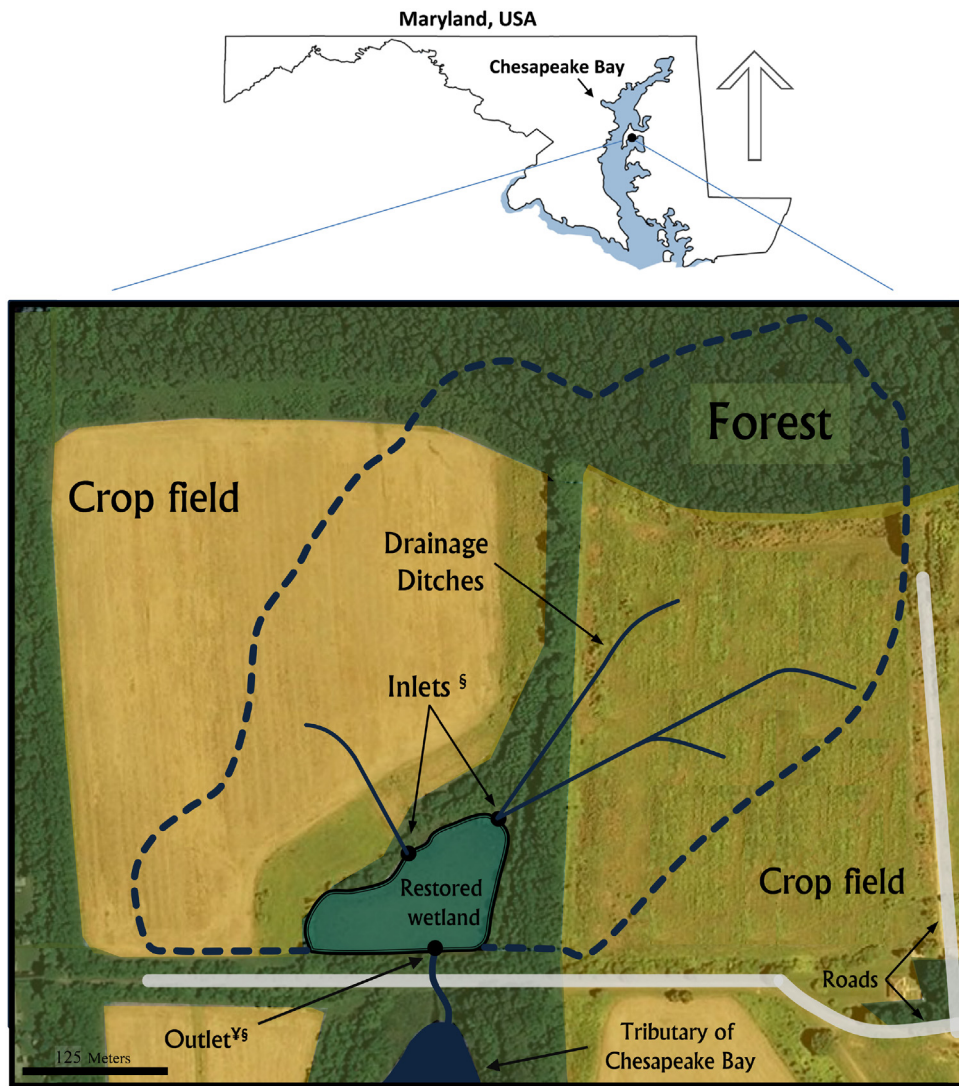
$$\alpha_M = 0.17 U_{10} \left(\frac{Sc_M}{600} \right)^{-0.5} \quad (22)$$

where α_M has a unit of cm h⁻¹, Sc_M is Schmidt number of methane in a given temperature (see Appendix A for details) and U_{10} is wind speed at 10 meters above water (m s⁻¹) (Riera et al., 1999; Wanninkhof et al., 2009).

3. Model assessment

3.1. Study area and input data

The developed model was applied to a study wetland with approximately two years of monitored flow and water quality data, described thoroughly by Jordan et al. (2003). The study site is a small restored wetland located on Kent Island, Maryland (Fig. 2). During the two year sampling period, the study wetland had an average area of 1.3 ha and drained a 14 ha watershed that was mainly covered by crop fields (82%) and forest (18%). The study wetland was restored from an artificially drained cropland by the Chesapeake Wildlife Heritage with the intention to provide wildlife habitat and improve the quality of runoff from surrounding crop fields. A maximum 90% of the wetland surface was covered by emergent vegetation during growing season; this portion dropped to a minimum of 10% during non-growing season. Water entered the wetland through ditches draining surface runoff from surrounding catchment and outflowed via a standpipe connected to a 120° V-notch weir. The entire 1.3-ha area of the wetland was



[¶] Outflow structure consisted of a standpipe connected to a 120° V-notch weir.

[§] Automated samplers were installed to sample water entering and leaving the wetland.

Fig. 2. Study wetland and its watershed outlined by dashed lines (regenerated from [Jordan et al., 2003](#)). Located on Kent Island, MD (coordinates 38°56'20"N, 76°15'45"W), the wetland was monitored for flow and water quality constituents over a period of 2 years.

submerged and lacked well-defined flow channels when the water was deep enough to flow out of the weir. An impermeable layer of clay, laid within 0.5 m of soil surface during wetland restoration blocked groundwater exchanges and infiltration. Automated instruments were used to measure unregulated water inflows and to sample water entering and leaving the wetland from 8 May 1995 through 12 May 1997. Weekly (typically 5–8 days) flow averaged nitrate N, total ammonia N, organic N, inorganic P, and TSS and TOC (total organic carbon) concentrations in runoff were available from [Jordan et al. \(2003\)](#). Details of data collection and analysis can be found in [Jordan et al. \(2003\)](#).

To convert weekly average concentrations reported by [Jordan et al. \(2003\)](#) into daily values, we assumed that concentrations were constant over the given weekly periods. The dataset also contained periods where data were missing. We reconstructed the records during such periods by taking averages of the last available measurement before the gap and the first available measurement at the end of the gap. Sources for other input data (precipitation, temperature, etc.) used in the model could be found in [Kalin et al. \(2012\)](#) who validated the N and P cycles of WetQual model on the same

study wetland. Unfortunately the dataset does not include methane emission measurements, so we were not able to completely validate the methane component of the model. Yet, parameter values acquired from literature allowed us to perform a thorough sensitivity analysis on methane production and emission from the study wetland. [Fig. 3](#) exhibits the hydrology of the study wetland (inflow, outflow and average water depth) in addition to inflow concentrations of TOC to the study wetland from May 1995 to May 1997.

3.2. Numerical scheme verification

An explicit scheme with forward-difference approximation of the time derivatives was employed as a stable/efficient method for numerical integration. The named scheme was previously employed and explained by [Hantush et al. \(2012\)](#). The selected numerical integration time step is $\Delta t = 0.01$ day, however to save memory storage, results are aggregated to daily averages. [Hantush et al. \(2012\)](#) verified the used numerical approach by comparing model results with analytical solutions for simplified cases.

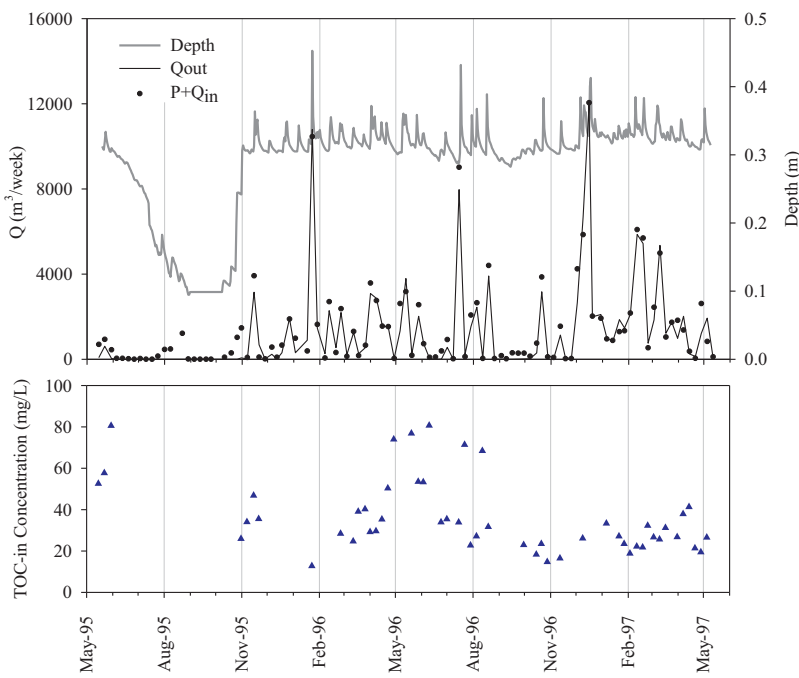


Fig. 3. Top panel: solid gray line presents average water depth (m) in study wetland; black dots show weekly inflow (Precipitation + inflow discharge aggregated over a week) and black solid line presents weekly outflow over the study period (m^3/week). Bottom panel: Measured concentration of TOC inflow (mg/L) to wetland over the study period.

However, in this study, we employed a secondary numerical structure to verify solutions provided by the explicit scheme. For the secondary numerical scheme, all equations contained within in the larger WetQual model (equations for nitrogen, phosphorus, carbon and sediment) were solved implicitly as coupled system of ordinary differential equations (ODEs) with central difference approximation. The secondary solution uses a time step of same length ($\Delta t = 0.01$ day), yet model takes about three times as long to run. Solutions provided by both methods were compared for different carbon constituents (DOC, LPOC, RPOC and CH_4). The differences between time series provided by both methods were indistinguishable for carbon pools within water and both oxidized and reduced soil layers. The perfect match between two solutions provided confidence and proof in effectiveness of the used explicit numerical scheme.

3.3. Uncertainty and sensitivity assessment

Generalized Likelihood Uncertainty Estimation (GLUE), introduced by Beven and Binley (1992), advocates the idea that there are always several different models and parameter sets for a single model that represent an observed natural process equally well. In other words, as Beven and Freer (2001) put it, “there are many different model structures and many different parameter sets within a chosen model structure that may be behavioral or acceptable in reproducing the observed behavior of a system”. Following this notion referred to as “Equifinality”, model calibration is not sought in the traditional way (i.e. finding an “optimum” parameter set), and rather, a group of parameter sets that generate model results consistent with observations are sought after. GLUE provides a simple uncertainty estimation method easily applicable to non-linear complex models. GLUE methodology is an extension to Generalized Sensitivity Analysis (GSA), first introduced by Spear and Hornberger (1980). Both GSA and GLUE are based upon Monte Carlo (MC) simulations. In this study, we employed a combination of both GLUE and GSA methods to simultaneously assess model prediction uncertainty and

quantitative sensitivity to input parameters. A brief portrayal of the GSA/GLUE methodology applied in this study is presented in Fig. 4. To apply GSA/GLUE method, we generated 100,000 statistically independent parameter sets, sampled randomly from previously defined distributions. The parameter distribution and their respective upper and lower bounds (quantities) are listed in Table 3. Such information was extracted from literature values/tabulations (e.g. Schnoor, 1996; Chapra, 1997; Di Toro, 2001; Reddy and DeLaune, 2008; Cerco and Cole, 1995; Ji, 2008) and authors' judgment. To perform MC simulations, the model was run 100,000 times, each time with one set of parameters to yield an ensemble of 100,000 time series for constituent concentrations. Two performance criteria were used to construct a likelihood function that evaluates the goodness of fit between model-predicted concentrations and observed data for each MC simulation. The likelihood function uses a combination of Mass Balance Error (MBE) and Nash-Sutcliffe efficiency (E_{ns}) (Kalin and Hantush, 2006) such that:

$$L_k = 0.5 \times (E_{ns} + \exp \left(\frac{-|\text{MBE}|}{100} \right)) \quad (23)$$

The likelihood function L can theoretically range between $-\infty$ and 1. Such a measure enables us capture goodness of fit for both average constituent concentrations and its variation over time. Following the methodology presented in Fig. 4, model parameter sets were sorted from largest to smallest respective likelihoods and the top 1000 datasets (top 1%) with the highest likelihoods were separated as behavioral dataset (B) from the rest of the parameter sets (non-behavioral datasets, B'). Special attention was given in selecting the cutoff limit for behavioral datasets. After special consideration, 1% limit was recognized as effectual cutoff limit, yet for the parameters to be selected as behavioral dataset, the respective model performance needed to yield a Nash-Sutcliffe efficiency larger than 0.7 ($E_{ns} > 0.7$) and a mass balance error smaller than 5% ($|\text{MBE}| < 5\%$). Given that the used measures have unequal domains, implementing such limits gives both measures more or less equal weights in the likelihood function. A simple weighing average method was used to yield best estimations for WetQual-C

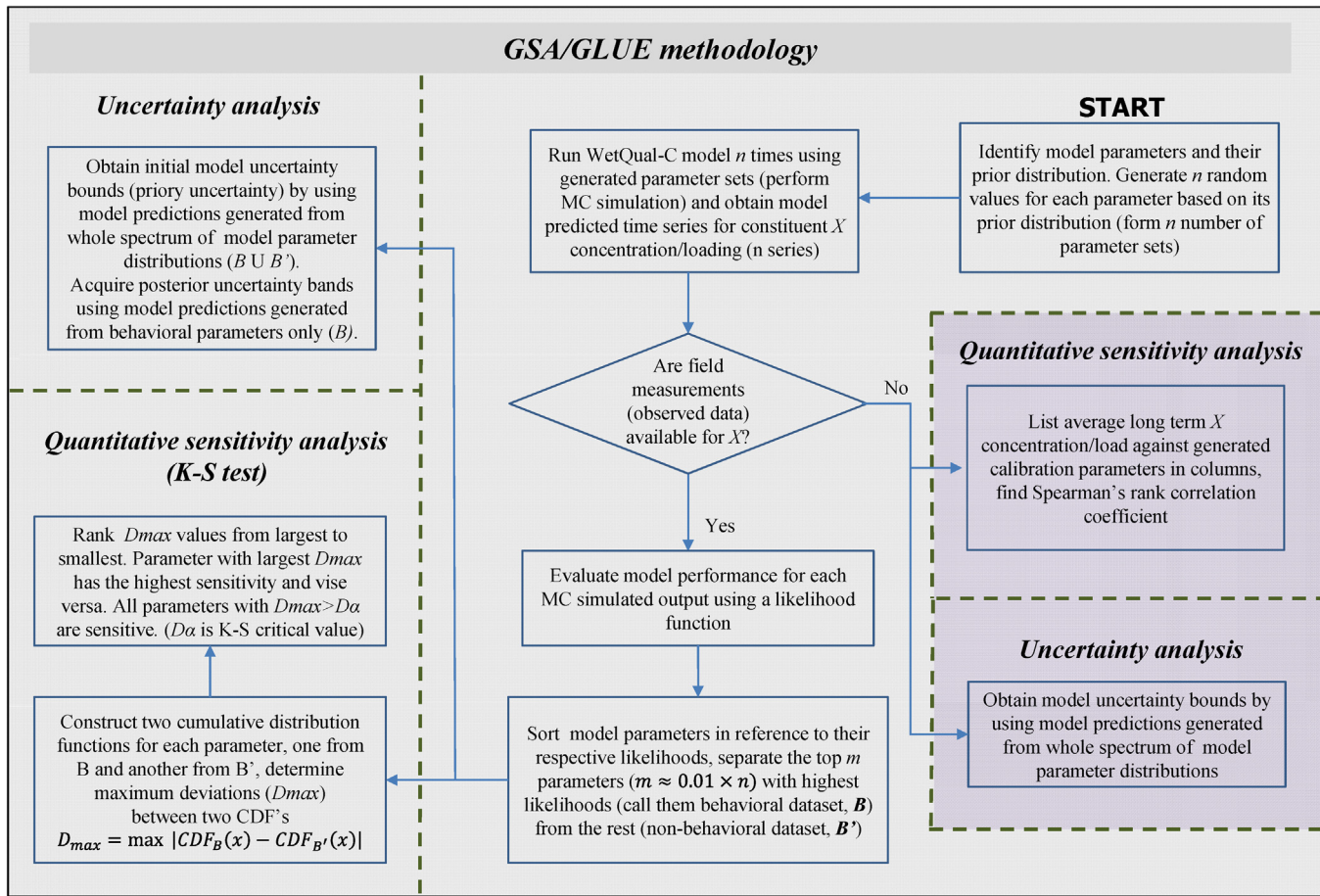


Fig. 4. Stepwise flowchart to GSA/GLUE methodology applied in this study.

model parameters. Behavioral parameter values were given a weight proportional to their respective likelihood and averaged as follows:

$$x' = \frac{\sum_{i=1}^n (e^{L_k-1} x_i)}{\sum_{i=1}^n e^{L_k-1}} \quad (24)$$

where x' is best estimate for parameter x , L_k is the corresponding likelihood from the i th model run of the MC simulation, n is the total number of MC simulations, and x_i is the generated value of parameter x in i th parameter set.

Subsequently, quantitative sensitivity analysis was performed using Kolmogorov-Smirnov test (Massey Jr, 1951) to reveal the most sensitive parameters. Kolmogorov-Smirnov test is a non-parametric test that is used to quantify a distance between the reference cumulative distribution function (CDF) – generated from non-behavioral parameter values or B' – and posterior CDF of a parameter generated from behavioral datasets (or B). If such distance – referred to as D_{max} – is significant at 5% confidence level, the parameter is declared sensitive. Prior and posterior prediction uncertainty were next obtained by using model predictions generated respectively from the whole spectrum of model parameter distributions ($B \cup B'$), and from behavioral parameters only (B).

For simulated constituents that do not have equivalent field measurements (like methane in this study), a simple method for determining most sensitive parameters quantitatively is to use Spearman's rank correlation coefficient (Saltelli and Sobol, 1995). In this method the strength of monotonic relationship (linear correlation) between the ranks of each input (parameter values) and output (simulated constituent concentration) is measured.

Spearman's correlation coefficient ranges from -1 to 1, and a negative correlation between a parameters and constituent concentration imposes an inverse relationship between the two.

4. Results and discussion

As stated before, the measured observed data is limited to flow and weekly averaged incoming and outflowing TOC concentration measurements. CO₂ and CH₄ emissions were not monitored on the study wetland. Thus, in the following sections, we will demonstrate model performance, uncertainty and parameter sensitivity on TOC export. CH₄ component of the model was examined thoroughly by performing rank correlation sensitivity analysis. At the end, carbon budgets for the study wetland are presented. Many of the equations presented earlier require concentration of NO₃ in water and sediment layers as input. Kalin et al. (2012) validated the nitrate component of the WetQual model, therefore model simulated concentrations of NO₃ were used when required.

4.1. TOC export

Simulated TOC concentrations are obtained by lumping model generated concentrations of DOC, LPOC and RPOC at each time step. Although model required separate inflow concentrations for LPOC, RPOC and DOC, such information was not available for the case study wetland; instead, the lumped amount of the three pools (TOC) was measured at wetland inlets. We disaggregated the sum into three separate pools by relying on model fine tuning and information provided by Jordan et al. (1999). Model fine tuning exposed that best fits to observed data are achieved when roughly 89% of

Table 3

Model parameters considered random and their best estimates based on TOC export.

| Parameters | Distribution (literature) ^a | Min(a) (literature) ^a | Max(a) (literature) ^a | Best estimates for TOC model | Best estimates for ON model ^b |
|-----------------------|--|----------------------------------|----------------------------------|------------------------------|--|
| H (cm) | U^c | 5.00 | 50.00 | 23.94 | 21.20 |
| θ | U | 1.15 | 1.35 | 1.307 | 1.10 |
| k_{ga} (d^{-1}) | log- N^d | 0.01 | 0.2 | 0.00143 | 0.0014 |
| k_{gb} (d^{-1}) | log- N | 0.01 | 0.2 | 0.00142 | 0.0014 |
| ρ_s (g/cm^3) | U | 1.5 | 2.2 | 2.01 | 2.01 |
| v_s (cm/d) | log- N | 0.025 | 25 | 1.779 | 2.34 |
| v_b (cm/d) | U | 0.000274 | 0.006575 | 0.0034 | 0.0035 |
| φ | U | 0.5 | 0.9 | 0.668 | 0.684 |
| φ_w | U | 0.65 | 0.95 | 0.8768 | 0.865 |
| v_r (mm/yr) | log- N | 0.0146 | 8.74 | 0.029 | 0.024 |
| a_{ca} (gC/gChl) | U | 15 | 160 | 86.174 | |
| f_{al} | U | 0.01 | 0.99 | 0.423 | |
| f_{aR} | U | 0.01 | 0.99 | 0.421 | |
| f_{aD} | U | 0.01 | 0.33 | 0.156 | |
| f_{bL} | U | 0.01 | 0.99 | 0.430 | |
| f_{bR} | U | 0.04 | 0.99 | 0.412 | |
| f_{bD} | U | 0.01 | 0.33 | 0.158 | |
| k_L (d^{-1}) | log- N | 0.000001 | 0.0001 | 0.0000135 | |
| k_R (d^{-1}) | log- N | 0.0000001 | 0.00001 | 0.00000127 | |
| K_O (mg/lit) | U | 0.2 | 1.00 | 0.5453 | |
| K_O^{in} (mg/lit) | U | 0 | 0.51 | 0.2732 | |
| K_N (mg/lit) | log- N | 0.004 | 0.36 | 0.0519 | |
| K_N^{in} (mg/lit) | log- N | 0.002 | 0.18 | 0.0271 | |
| k_D^1 (d^{-1}) | U | 0.0015 | 0.4 | 0.2174 | |
| k_D^2 (d^{-1}) | U | 0.001 | 0.16 | 0.1086 | |
| k_D^3 (d^{-1}) | U | 0.0005 | 0.08 | 0.0276 | |
| β_{D1} (cm/d) | - ^e | 0.85 | 109.02 | 27.87 | |
| k_M^1 (d^{-1}) | U | 0.001 | 0.25 | – | |
| k_M^2 (d^{-1}) | U | 0.001 | 0.08 | – | |
| f_{bw} | U | 0.4 | 0.7 | 0.547 | |
| R_v | log- N | 0.001 | 10.00 | – | |
| β_{MI} (cm/d) | – | 0.92 | 131.57 | – | |

^a The selected ranges (Min, Max) and distributions for the listed parameters/coefficients are extracted from literature and expert knowledge (e.g. Schnoor, 1996; Chapra, 1997; Di Toro, 2001; Reddy and DeLaune, 2008; Cerco and Cole, 1995; Ji, 2008). Also see Hantush et al. (2012) and Kalin et al. (2012) for list of other parameters (regarding N + P cycles) in WetQual model.

^b Values in last column (Best estimates for ON model) are from Kalin et al. (2012).

^c Uniform distribution.

^d Log-normal distribution. Lower and upper bounds in log-N distributions refer to values corresponding to probabilities of 0.1% and 99.9%. Grey lines mark parameters that are shared with N cycling in WetQual model.

^e No specific distribution assigned.

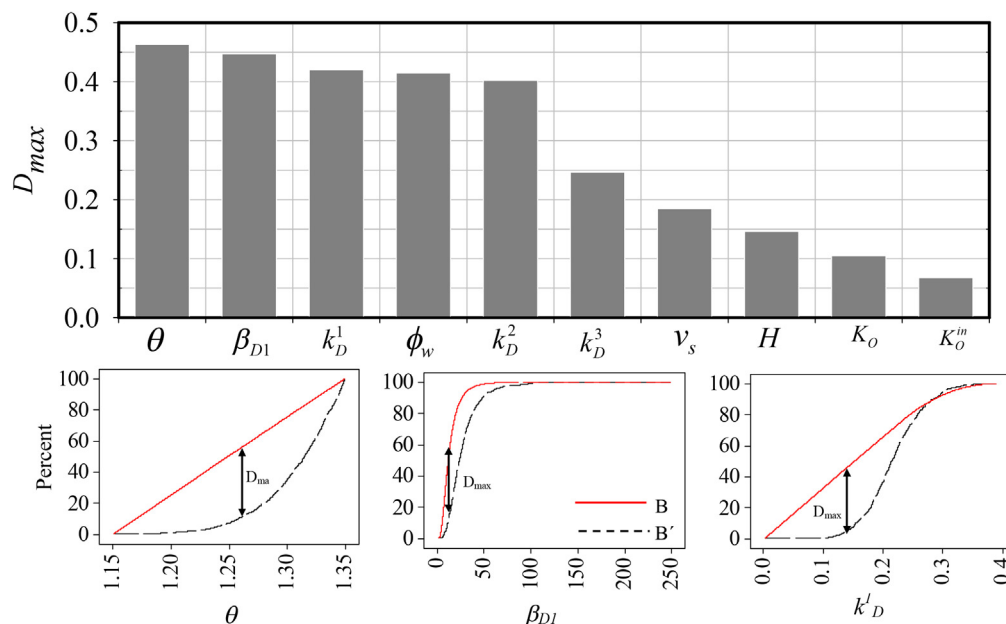


Fig. 5. Top: Summary of the K-S test and order of sensitivities based on TOC export for the whole study period. All parameters presented in figure have p -values smaller than 0.0003 thus declared sensitive. Bottom: Cumulative distribution functions (CDFs) of three most sensitive parameters. CDF of behavioral (B) and non-behavioral parameter sets have a wide gap between them, revealing model's high sensitivity to that parameter.

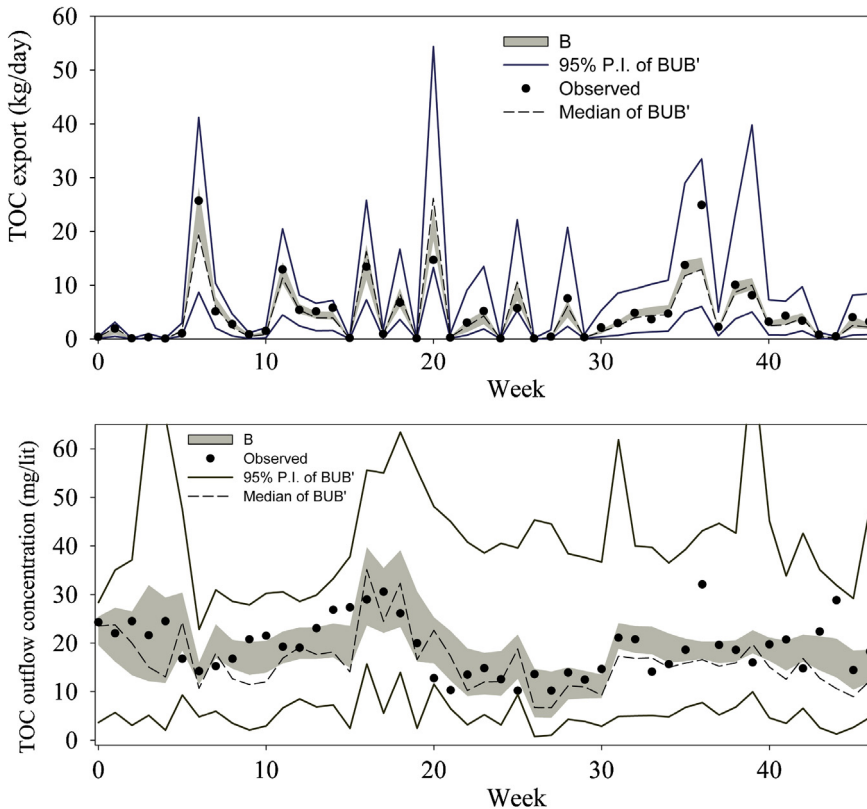


Fig. 6. Model generated 95% prediction interval (P.I.) from 100,000 MC simulations versus field observations. B in figure represents behavioral datasets whereas B' exhibits non-behavioral datasets. Dashed line presents the median values for BUB'. To avoid gaps in figure, some weeks with missing observed data were ignored. Last data point on the plots, week 47 corresponds to the last week of the 2 year simulation period.

the inflowing TOC is considered as DOC. The study by Jordan et al. (1999), which performed an experimental study on the same study wetland between 1994 and 1995, supports this finding by stating that DOC constituted over 75% of TOC entering the study wetland between 1994 and 1995. Model performance showed small sensitivity to how the remaining 11% of TOC inflow was distributed between LPOC and RPOC pools, thus the remainder was split equally between the two pools.

4.1.1. Quantitative sensitivity analysis (K-S test)

Fig. 5 presents results of the K-S test performed on model parameters. 10 model parameters were identified as sensitive using the test (top panel), in which all had small p -values ($p < 0.0003$). Bottom panel of Fig. 5 shows the maximum gap (D_{\max}) between cumulative distribution functions of behavioral and non-behavioral data sets for the three top sensitive parameters. Most sensitive parameter was identified as θ , imposing the notion that temperature plays a significant role in regulating TOC export. Knowing that TOC pool is mostly comprised of DOC (~90%), and considering the repeated effects of temperature related to DOC transfer (diffusion), origination (LPOC, RPOC hydrolysis) and conversion (aerobic/anaerobic decomposition), it is not unexpected to see θ as a sensitive parameter. Four other parameters in order of sensitivity were β_{D1} , k_D^1 , φ_w and k_D^2 . Given the fact that D_{\max} of first five parameters are considerably close to each other ($0.4 < D_{\max} < 0.47$), we can state that the most equally important processes governing TOC export in this studied wetland system are diffusion of DOC, aerobic decomposition and denitrification of DOC. Similar to θ , φ_w (fourth in order of sensitivity) does not present a specific process, rather it accounts for plant biomass and other debris obstructing flow and flow-accessibility in wetland water pool. The second half of sensitive

parameters (last five) include k_D^3 , v_s , H , K_O and K_O^{in} , conveying secondary importance of methanogenesis, settling, thickness of active sediment layer and oxygen concentration on TOC export.

4.1.2. Parameter estimation

Based on the averaging method explained earlier (Section 3.3), best estimates for parameters involved in TOC export modeling were calculated (Table 3). Presenting a single value for a parameter might promote the concept of calibration and seem against the notion of equifinality, yet our intention of presenting such values is rather to give the reader estimates of mean parameter values. This

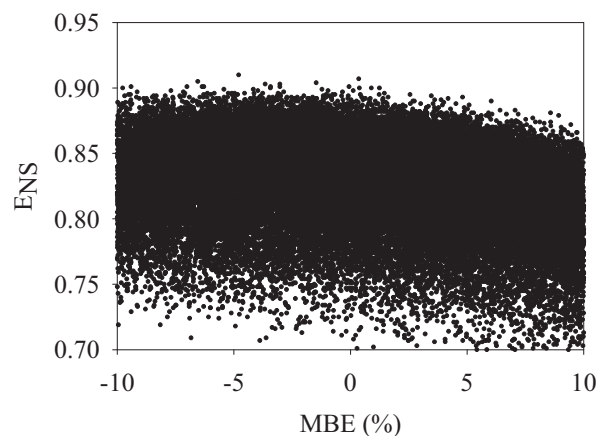


Fig. 7. Dotty plot exhibiting ENS vs. MBE. The relative scatterings of dots over the graph reveal non-independence of the two performance criteria.

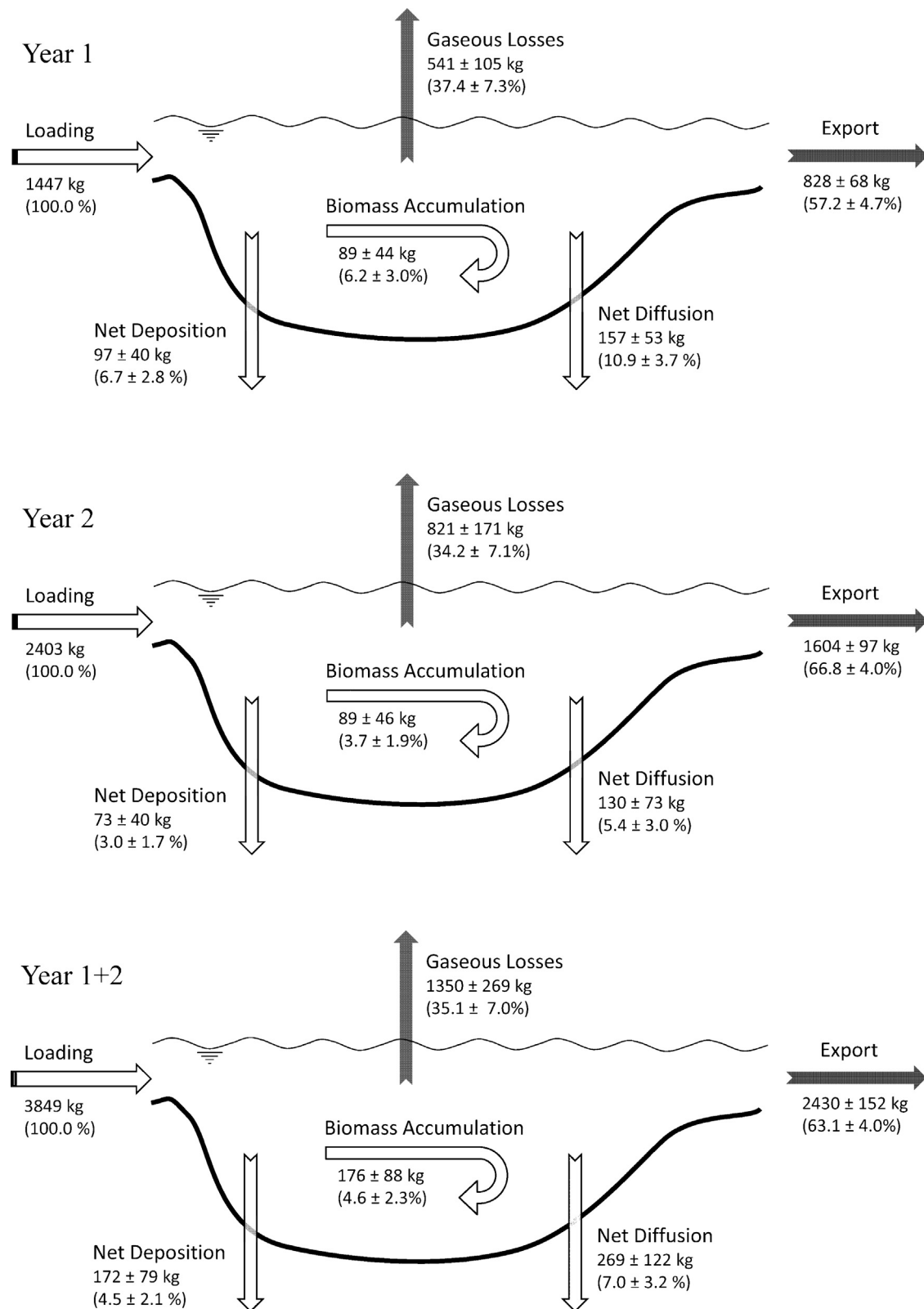


Fig. 8. Carbon net mass exchanges and export in study wetland over year 1, year 2 and the whole simulation period. Figure presents mass of inflowing OC (kg), and OC lost to outflow, removal and retention processes in the study wetland. Values in parentheses are mass normalized with input loading. To account for simulation uncertainty, absolute and normalized budget values are presented \pm one standard deviation of behavioral predictions. Gaseous losses account for mass of OC turned into CO_2 or CH_4 via microbial activities.

practice also allows us to compare best estimates obtained in this study to ones obtained in Kalin et al. (2012) for organic nitrogen (ON). These shared parameters are marked in grey in Table 3. As no observed data was available for methane emission, best estimates

for some methane related parameters could not be obtained. In general, calculated best estimates for shared parameters are reasonably close to estimations obtained from ON simulations. As explained previously, best estimate for θ obtained for carbon export is 16%

larger than the value estimated for ON, expressing higher sensitivity of C cycling to temperature variation.

4.1.3. Model performance and uncertainty analysis

Fig. 6 demonstrates the comparison between field measured TOC export (top) and outflow concentrations (bottom) with model results, generated from the behavioral and non-behavioral MC simulations. As declared earlier, there are periods with no observed data (no field measurements). For purpose of presentation, we discarded those absent weeks in order not to leave any breaks, thus the horizontal axes in the figures do not reflect consecutive weeks. As appears in **Fig. 6**, model performs decently in predicting TOC export from case study wetland with relatively small uncertainty. Average L_k , E_{ns} and MBE for behavioral simulations concerning TOC export are respectively equal to 0.93, 0.87 and 0.81%. 95% prediction intervals at the top panel of **Fig. 6** disclose that uncertainty is highest when TOC export is at a local peak. These peaks happen to coincide with peaks in outflow (not shown), suggesting that highest model uncertainty can be expected when flow is high. At low flows, when TOC export is minimal, model has a very narrow uncertainty band (both prior and posterior). The uncertainty for behavioral simulations is relatively small. The bottom panel reveals that behavioral model uncertainty is wider when concentration is simulated. The median time series for MC simulations performed in this study are shown in **Fig. 6** with dashed lines. As can be seen, the median time series on both panels have close agreements with observations.

The defined likelihood measure used in this study benefits from two discrete goodness of fit criteria, namely Mass Balance Error (MBE) and Nash-Sutcliffe Efficiency (E_{ns}). Both measures offer valuable information on how well model can mimic the dynamics of carbon cycling in flooded wetlands. E_{ns} measures model goodness of fit by comparing both shape and volume of simulated OC export profile versus field observations, whereas MBE evaluates model fitness based on relative percentage difference between the average of two profiles (simulated and observed) over simulation period (Arabi et al., 2007; Dongquan et al., 2012). Indeed, combining fitness measures only becomes rewarding when each measure offers independent information, in other words fitness measures ought to be independent from one another. We checked the correlation between MBE and E_{ns} values obtained from comparing model simulations of TOC export with field observations. The dotty plot in **Fig. 7** has E_{ns} on vertical axis and MBE on horizontal axis for simulations which yielded $E_{ns} > 0.7$ and $|MBE| < 5\%$. Dots scatter all around the plot suggest a non-existent, or rather a weak correlation ($R^2 = 0.05$, $p \geq 0$) between the two measures, confirming their independence, thus supporting the use of both fitness measures to distinguish behavioral from non-behavioral parameter sets.

4.2. Methane emission

Methane and carbon dioxide emissions were not monitored at the study wetland. This prohibits verifying the methane component of the model against observed data. However, as pointed out earlier, we scrutinized the methane module via testing its sensitivity to model parameters.

Spearman's rank correlation test (**Table 4**) revealed that thickness of active sediment (H) has a high positive correlation ($R = 0.76$) with amount of modeled methane emission. Methanogenesis rate in anaerobic soil (k_D^3) also appeared sensitive ($R = 0.33$) and positively correlated with methane emission. Third sensitive parameter with strong positive correlation ($R = 0.29$) appeared as nitrate inhibition factor (K_N^{in}). This means that model allows for more methane production when K_N^{in} is set to higher concentrations. Methane component of the model did not show strong sensitivity to other model parameters.

Table 4

Rank correlation coefficients (%) of model outputs versus model parameters for methane emission.

| Parameter | Rank correlation |
|--------------|------------------|
| H | 0.76 |
| k_D^3 | 0.33 |
| K_N^{in} | 0.29 |
| β_{M1} | -0.10 |
| ϕ | -0.08 |
| θ | 0.07 |
| ϕ_w | -0.05 |
| K_O | 0.05 |
| K_O^{in} | 0.03 |
| k_M^1 | -0.01 |
| k_M^2 | -0.01 |
| ρ_s | -0.01 |

4.3. Carbon mass exchanges and exports

Fig. 8 presents the carbon mass exchanges and exports for the study wetland, averaged over behavioral model outputs in year 1, year 2 and the whole simulation period (year 1 + year 2). Over the two year study period, 3849 kg of allochthonous organic carbon was washed into the wetland through inflow. In addition, 176 ± 88 kg of atmospheric C was fixed by plants over the simulation period. Over the two year period, 1350 ± 269 kg of OC (equivalent to $35.1 \pm 7.0\%$ of OC loading) was removed via microbial decomposition processes and emitted to the atmosphere (Gaseous loss in **Fig. 8**). It should be noted that at current state, WetQual-C does not trace CO_2 transport and consumption. For that reason, the reported gaseous loss averages were obtained by adding masses of CO_2 and CH_4 produced from aerobic and anaerobic microbial oxidation of DOC. Diffusion of DOC to soil layers retained 269 ± 122 kg ($7.0 \pm 3.2\%$ of OC loading) and a relatively small amount (172 ± 79 kg, equivalent to $4.5 \pm 2.1\%$ of OC load) was retained in the soil as a result of settling. In the second year, wetland received around 66% (1000 kg) more OC than year 1. This could be traced back to a long dry period at the beginning of year 1 (see **Fig. 3**) where hydrologic import to the wetland was limited. Reduced inflow discharge and loading in year 1 allowed for higher percentage of OC retention/removal compared to second year. According to **Fig. 8**, in year 1, equivalent to $42.8 \pm 4.7\%$ of the OC loading was removed by the study wetland whereas for year 2, this ratio was $33.2 \pm 4.0\%$. By comparison Jordan et al. (2003) measured 41% and 30% removal of TOC for years 1 and 2, respectively.

5. Summary and conclusion

In this paper, we described development and validation of WetQual-C, a process based mathematical model for carbon cycling in flooded wetlands. The model is an extension to WetQual model (Hantush et al., 2012), a previously developed wetland nitrogen and phosphorus cycling model. WetQual-C reflects various biogeochemical interactions affecting C cycling in wetlands, and is capable of simulating the dynamics of OC retention, OC export and GHG emissions all at once. WetQual-C is coupled with other interrelated geochemical cycles (i.e. nitrogen and oxygen) and fully reflects the dynamics of the thin oxidized zone at wetlands soil-water interface, and the oxidation-reduction reactions taking place within that zone. A thorough sensitivity and uncertainty analysis was performed on model components to evaluate its credibility using field collected data from a small wetland.

Model showed a narrow behavioral uncertainty predicting TOC export however, overall model uncertainty peaked substantially when outflow was high. Overall, model performed well in capturing TOC export fluctuations and dynamics from the study wetland. Model appears to be more reliable and less uncertain when it is

predictions on TOC export is used; nevertheless, model performance on concentration simulations was shown to be relatively acceptable too.

The presented model in this study is a process based model, i.e. most parameters and constants have physical meanings. Through lab and in situ experiments, most variables could potentially be estimated. Although the number of parameters used in WetQual-C might appear disproportionate, if water quality is monitored (even for a short period of time), least sensitive parameters could easily be identified via sensitivity analysis, and fixed at their average values. In case observed data are not available for the study wetland, model users can still benefit from the median results of the MC simulation time series.

Over the period of 2 years, the study wetland removed equivalent to $35.1 \pm 7.0\%$ of the OC carbon intake via OC decomposition, and retained equivalent to $11.5 \pm 5.3\%$ mainly through DOC diffusion to sediment. Thus, the study wetland appeared as a carbon sink rather than source and proved its purpose as a relatively effective and low cost mean for improving water quality. As WetQual-C was intended for fresh water wetlands, it does not account for methane removal by anaerobic oxidation processes other than denitrification. This can be a limitation if WetQual-C is applied to salt water wetlands where sulfate and other minerals are abundant.

Since hydrology was an input to the model, we did not consider uncertainties related to flow measurements. Uncertainty in field measurements (input uncertainty) was not assessed either, assuming that field measurements are accurate and not too deviant. Such additional uncertainties were ignored due to lack of information on measurement deviations; however, if they were counted for, the marks representing observed data (black dots in Fig. 6) would have appeared with uncertainty bands, enabling us to compare model uncertainty with input uncertainty.

The process of parting behavioral parameter sets from non-behavioral ones is indeed exceedingly delicate and one should pay particular attention to selecting right likelihood measures for such purposes. Faulty, imprecise uncertainty and sensitivity analysis is a very probable consequence of relying on improper likelihood measures for testing model fitness. In this study, we defined a new likelihood measure that combines two discrete goodness of fit criteria, namely Mass Balance Error and Nash-Sutcliff Efficiency. By means of a dotty plot (Fig. 7), it was revealed that there was a weak correlation between the two goodness of fit measures, confirming their independence. This independence promises that each measure offers unique information, thus supporting the use of both fitness measures for distinguishing behavioral from non-behavioral parameter sets.

Acknowledgements

The U.S. Environmental Protection Agency through its Office of Research and Development partially funded and collaborated in the research described here under contract (EP08C000066) with Auburn University, School of Forestry and Wildlife Sciences. It has not been subject to the Agency review and therefore does not necessarily reflect the views of the Agency, and no official endorsement should be inferred.

Appendix A. Temperature dependence

- Arhenius equation (Chapra, 1997; Schnoor, 1996) is used to describe dependence of several reaction rates and model variables to temperature variation:

$$k_T = k_{20} \theta^{T-20} \quad (\text{A.1})$$

where T is temperature expressed in $^{\circ}\text{C}$; θ is a constant temperature coefficient; and k_{20} is the rate constant at the reference temperature 20°C . θ is usually greater than 1 and can be considered as a calibration coefficient. k_{da} , k_{db} , k_L , k_R , k_D^1 , k_D^2 , k_D^3 , K_N^{in} , K_O^{in} , K_N , K_O , k_M^1 , k_M^2 are among the variables and rates adjusted for temperature.

- Diffusivity of DOC in open water, D_D^* (unit: $\text{cm}^2 \text{d}^{-1}$) is adjusted for temperature using an average form suggested by Boudreau (1997).

$$D_D^* = 0.0864(9.5 + 0.3319T) \quad (\text{A.2})$$

where T is water temperature in K.

D^σ , defined as diffusivity of CH_4 in air ($\text{m}^2 \text{s}^{-1}$), is adjusted for temperature following Tang et al. (2010):

$$D^\sigma = 1.9 \times 10^{-5} \times \left(\frac{T}{298} \right)^{1.82} \quad (\text{A.3})$$

where T is ambient air temperature in K.

- Equation for methane free water diffusion coefficient, D_M^* (unit: $\text{cm}^2 \text{d}^{-1}$) is given by (Arah and Stephen, 1998; Tang et al., 2010):

$$D_M^* = 1.5 \times 10^{-9} \times \left(\frac{T}{298} \right) \quad (\text{A.4})$$

- Wania et al. (2010) provided a temperature dependent relationship for methane Bunsen solubility coefficient (S_B) by fitting a second order polynomial to observations provided by Yamamoto et al. (1976):

$$S_B = 0.05708 - 0.001545T + 0.00002069T^2 \quad (\text{A.5})$$

where T is water temperature in K.

- Equilibrium concentration of CH_4 in atmosphere, C^* [ML^{-3}] can be obtained from Henry's law. Following equation describes C^* when dependency of Henry's coefficient to temperature is considered (Sander, 1999):

$$C^* = 1.4 \times 10^{-3} \exp \left[-1700 \left(\frac{1}{T} - \frac{1}{298} \right) \right] \times p_{\text{CH}_4} \quad (\text{A.6})$$

where C^* has a unit of mol L^{-1} and T is ambient air temperature in K. p_{CH_4} is atmospheric partial pressure of methane, assigned a constant value of 1.7×10^{-6} atm (Wania et al., 2010).

- Following Rietta et al. (1999) and Wania et al. (2010), a third order polynomial, fitted to observations obtained by Jähne et al. (1987), was used to describe temperature dependency of methane Schmidt number:

$$Sc_M = 1898 - 110.1T + 2.834T^2 - 0.02791T^3 \quad (\text{A.7})$$

where T is water temperature in $^{\circ}\text{C}$.

Appendix B. Diffusive mass transfer coefficients

Diffusive mass transfer coefficients of β_D and β_M are calculated using a two-layer approach similar to Hantush et al. (2012). Assuming linear variation of concentration between layers, for substance x , effective mass transfer coefficient between water and aerobic sediment, β_{x1} is given by

$$\beta_{x1} = \frac{2\phi_w \phi \tau D_x^*}{\phi \tau h + \phi_w l_1}, \quad x = D, M \quad (\text{B.1})$$

Similarly, β_{x2} (effective mass transfer coefficient between aerobic and anaerobic sediment layers) is

$$\beta_{x2} = \frac{2\phi\tau D_x^*}{l_1 + l_2}, \quad x = D, M \quad (\text{B.2})$$

where, D_x^* is free-water diffusion coefficient for substance x [L^2T^{-1}]; and τ is tortuosity of sediment (Refer to Table 1 for definition of other parameters).

References

- Arabi, M., Govindaraju, R.S., Hantush, M.M., 2007. A probabilistic approach for analysis of uncertainty in the evaluation of watershed management practices. *Journal of Hydrology* 333, 459–471.
- Arah, J., Stephen, K., 1998. A model of the processes leading to methane emission from peatland. *Atmospheric Environment* 32, 3257–3264.
- Aselmam, I., Crutzen, P.J., 1989. Global distribution of natural freshwater wetlands and rice paddies: their net primary productivity, seasonality and possible methane emissions. *Journal of Atmospheric Chemistry* 8, 307–358.
- Barker, J., Fritz, P., 1981. The occurrence and origin of methane in some groundwater flow systems. *Canadian Journal of Earth Sciences* 18, 1802–1816.
- Beven, K., Binley, A., 1992. The future of distributed models: model calibration and uncertainty prediction. *Hydrological Processes* 6, 279–298.
- Beven, K., Freer, J., 2001. Equifinality, data assimilation, and uncertainty estimation in mechanistic modelling of complex environmental systems using the GLUE methodology. *Journal of Hydrology* 249, 11–29, [http://dx.doi.org/10.1016/S0022-1694\(01\)00421-8](http://dx.doi.org/10.1016/S0022-1694(01)00421-8).
- Boudreau, B.P., 1997. *Diagenetic Models and Their Implementation: Modelling Transport and Reactions in Aquatic Sediments*. Springer.
- Bradford, M., Ineson, P., Wookey, P., Lappin-Scott, H., 2001. Role of CH_4 oxidation, production and transport in forest soil CH_4 flux. *Soil Biology and Biochemistry* 33, 1625–1631.
- Byrnes, B., Austin, E., Tays, B., 1995. Methane emissions from flooded rice soils and plants under controlled conditions. *Soil Biology and Biochemistry* 27, 331–339.
- Canário, J., Vale, C., Nogueira, M., 2008. The pathway of mercury in contaminated waters determined by association with organic carbon (Tagus estuary, Portugal). *Applied Geochemistry* 23, 519–528.
- Cerci, C.F., Cole, T., 1995. User's Guide to the CE-QUAL-ICM Three-dimensional Eutrophication Model: Release Version 1.0. US Army Engineer Waterways Experiment Station.
- Chan, A., Parkin, T., 2000. Evaluation of potential inhibitors of methanogenesis and methane oxidation in a landfill cover soil. *Soil Biology and Biochemistry* 32, 1581–1590.
- Chapra, S.C., 1997. *Surface Water-Quality Modeling*. McGraw-Hill, New York.
- Chow, A.T., Tanji, K.K., Gao, S., 2003. Production of dissolved organic carbon (DOC) and trihalomethane (THM) precursor from peat soils. *Water Research* 37, 4475–4485.
- Cui, J., Li, C., Sun, G., Trettin, C., 2005. Linkage of MIKE SHE to Wetland-DNDC for carbon budgeting and anaerobic biogeochemistry simulation. *Biogeochemistry* 72, 147–167.
- Denman, K., Brasseur, G., Chidthaisong, A., Ciais, P., Cox, P., Dickinson, R., Hauglustaine, D., Heinze, C., Holland, E.J., et al., 2007. Couplings Between Changes in the Climate System and Biogeochemistry, in: Solomon et al. (2007). pp. 499–588.
- Di Toro, D.M., 2001. *Sediment Flux Modeling*. Wiley-Interscience, New York.
- Dongquan, Z., Jining, C., Haozheng, W., Qingyuan, T., 2012. Application of a sampling based the combined objective to parameter identification and uncertainty analysis of an urban rainfall-runoff modeling. *Journal of Irrigation and Drainage Engineering*.
- Hantush, M.M., Kalin, L., Isik, S., Yucekaya, A., 2012. Nutrient dynamics in flooded wetlands: I. Model development. *Journal of Hydrologic Engineering*, [http://dx.doi.org/10.1061/\(ASCE\)HE.1943-5584.0000741](http://dx.doi.org/10.1061/(ASCE)HE.1943-5584.0000741).
- Hedges, J., Keil, R., Benner, R., 1997. What happens to terrestrial organic matter in the ocean? *Organic Geochemistry* 27, 195–212.
- Jähne, B., Heinz, G., Dietrich, W., 1987. Measurement of the diffusion coefficients of sparingly soluble gases in water. *Journal of Geophysical Research* 92, 10710–10767, 10776.
- Ji, Z.-G., 2008. *Hydrodynamics and Water Quality: Modeling Rivers, Lakes, and Estuaries*. Wiley-Interscience.
- Jordan, T.E., Pittek, M.A., Hofmockel, K.H., Whigham, D.F., 2003. Nutrient and sediment removal by a restored wetland receiving agricultural runoff. *Journal of Environmental Quality* 32, 1534–1547.
- Jordan, T.E., Whigham, D.F., Hofmockel, K., Gerber, N., 1999. Restored Wetlands in Crop Fields Control Nutrient Runoff. *Nutrient Cycling and Retention in Natural and Constructed Wetlands*. Backhuys Publishers, The Netherlands, pp. 49–60.
- Kalin, L., Hantush, M.M., 2006. Hydrologic modeling of an eastern Pennsylvania watershed with NEXRAD and rain gauge data. *Journal of Hydrologic Engineering* 11, 555–569.
- Kalin, L., Hantush, M.M., Isik, S., Yucekaya, A., Jordan, T., 2012. Nutrient dynamics in flooded wetlands: II. Model evaluation. *Journal of Hydrologic Engineering*, [http://dx.doi.org/10.1061/\(ASCE\)HE.1943-5584.0000750](http://dx.doi.org/10.1061/(ASCE)HE.1943-5584.0000750).
- Kayranli, B., Scholz, M., Mustafa, A., Hedmark, Å., 2010. Carbon storage and fluxes within freshwater wetlands: a critical review. *Wetlands* 30, 111–124.
- Kellner, E., Baird, A., Oosterwoud, M., Harrison, K., Waddington, J., 2006. Effect of temperature and atmospheric pressure on methane (CH_4) ebullition from near-surface peats. *Geophysical Research Letters* 33, L18405.
- King, E., Bottrell, S., Sapsford, D., Raiswell, R., 2003. Modelling carbon fluxes in a constructed wetland. *Land Contamination and Reclamation* 11, 199–204.
- King, G., 1992. Ecological aspects of methane oxidation, a key determinant of global methane dynamics. *Advances in Microbial Ecology* 12, 431–468.
- Massey Jr, F.J., 1951. The Kolmogorov-Smirnov test for goodness of fit. *Journal of the American Statistical Association*, 68–78.
- Mitchell, D., 1994. Floodplain wetlands of the Murray-Darling Basin: management issues and challenges. *Murray-Darling Basin floodplain wetlands management*.
- Mitsch, W.J., Gosselink, J.G., 2007. *Wetlands*, 4th ed. Wiley, Hoboken, NJ, xi, 582 pp.
- Mitsch, W.J., Straškraba, M., Jrgensen, S.E., 1988. *Wetland Modelling (Developments in Environmental Modelling, v. 12)*. Elsevier Science Publishers.
- Penha-Lopes, G., Flindt, M.R., Ommen, B., Kristensen, E., Garret, P., Paula, J., 2012. Organic carbon dynamics in a constructed mangrove wastewater wetland populated with benthic fauna: a modelling approach. *Ecological Modelling* 232, 97–108.
- Reddy, K., Schipper, L.A., 1996. Determination of methane oxidation in the rhizosphere of Sagittaria lancifolia using methyl fluoride. *Soil Science Society of America Journal* 60, 611–616.
- Reddy, K.R., DeLaune, R.D., 2008. *Biogeochemistry of Wetlands: Science and Applications*, 1st ed. CRC Press, Taylor & Francis Group, Boca Raton, FL.
- Riera, J.L., Schindler, J.E., Kratz, T.K., 1999. Seasonal dynamics of carbon dioxide and methane in two clear-water lakes and two bog lakes in northern Wisconsin, USA. *Canadian Journal of Fisheries and Aquatic Sciences* 56, 265–274.
- Saltelli, A., Sobol, I.M., 1995. About the use of rank transformation in sensitivity analysis of model output. *Reliability Engineering & System Safety* 50, 225–239.
- Sander, R., 1999. *Compilation of Henry's Law Constants for Inorganic and Organic Species of Potential Importance in Environmental Chemistry*. Max-Planck Institute of Chemistry, Air Chemistry Department.
- Schnoor, J.L., 1996. *Environmental Modeling: Fate and Transport of Pollutants in Water, Air, and Soil*. John Wiley and Sons.
- Solomon, S., Qin, D., Manning, M., Chen, Z., Marquis, M., Averyt, K., Tignor, M., Miller, H., 2007. *Climate Change 2007: The Scientific Basis. Contribution of Working Group I to the Fourth Assessment Report of the Intergovernmental Panel on Climate Change*. Cambridge University Press, Cambridge.
- Spear, R., Hornberger, G., 1980. Eutrophication in pearl inlet—II. Identification of critical uncertainties via generalized sensitivity analysis. *Water Research* 14, 43–49.
- Steinberg, C., 2003. *Ecology of Humic Substances in Freshwaters: Determinants from Geochemistry to Ecological Niches*. Springer Verlag.
- Stern, J., Wang, Y., Gu, B., Newman, J., 2007. Distribution and turnover of carbon in natural and constructed wetlands in the Florida Everglades. *Applied Geochemistry* 22, 1936–1948.
- Tang, J., Zhuang, Q., Shannon, R., White, J., 2010. Quantifying wetland methane emissions with process-based models of different complexities. *Biogeosciences* 7, 3817–3837.
- Tranvik, L., Jansson, M., 2002. Climate change (Communication arising): terrestrial export of organic carbon. *Nature* 415, 861–862.
- Walter, B.P., Heimann, M., 2000. A process-based, climate-sensitive model to derive methane emissions from natural wetlands: application to five wetland sites, sensitivity to model parameters, and climate. *Global Biogeochemical Cycles* 14, 745–765.
- Wania, R., Ross, I., Prentice, I., 2010. Implementation and evaluation of a new methane model within a dynamic global vegetation model: LPJ-WHyMe v1.3.1. *Geoscientific Model Development* 3, 565–584.
- Wanninkhof, R., Asher, W.E., Ho, D.T., Sweeney, C., McGillivray, W.R., 2009. Advances in Quantifying Air-Sea Gas Exchange and Environmental Forcing, Annual Review of Marine Science, vol. 1. Annual Reviews, Palo Alto, pp. 213–244.
- Worrall, F., Burt, T., Shedd, R., 2003. Long term records of riverine dissolved organic matter. *Biogeochemistry* 64, 165–178.
- Yamamoto, S., Alcauskas, J.B., Crozier, T.E., 1976. Solubility of methane in distilled water and seawater. *Journal of Chemical and Engineering Data* 21, 78–80.
- Yu, K., Wang, Z., Chen, G., 1997. Nitrous oxide and methane transport through rice plants. *Biology and Fertility of Soils* 24, 341–343.
- Zhang, Y., Li, C., Trettin, C.C., Li, H., Sun, G., 2002. An integrated model of soil, hydrology, and vegetation for carbon dynamics in wetland ecosystems. *Global Biogeochemical Cycles* 16, 1061.
- Zhuang, Q., Melillo, J.M., Kicklighter, D.W., Prinn, R.G., McGuire, A.D., Steudler, P.A., Felzer, B.S., Hu, S., 2004. Methane fluxes between terrestrial ecosystems and the atmosphere at northern high latitudes during the past century: a retrospective analysis with a process-based biogeochemistry model. *Global Biogeochemical Cycles* 18, <http://dx.doi.org/10.1029/2004gb002239>, GB3010.
- Ziegler, S.E., Fogel, M.L., 2003. Seasonal and diel relationships between the isotopic compositions of dissolved and particulate organic matter in freshwater ecosystems. *Biogeochemistry* 64, 25–52.